

## Geology and Geochemistry of Lead-Zinc Mineralization in Ameri, Southeastern Nigeria

\*<sup>1</sup>Segun, A.B., <sup>1</sup>Jatau. B. S., <sup>1</sup>Tanko, I. Y.

<sup>1</sup>Department of Geology, Nasarawa State University, Keffi, Nigeria

doi: <https://doi.org/10.37745/bjesr.2013/vol12n25281>

Published June 15, 2024

**Citation:** Segun, A.B., Jatau. B. S., Tanko, I. Y. (2024) Geology and Geochemistry of Lead-Zinc Mineralization in Ameri, Southeastern Nigeria, *British Journal of Earth Sciences Research*, 12 (2),52-81

**ABSTRACT:** *The Geology and geochemistry of Lead-Zinc Mineralization has been carried out in parts of Ameri, South eastern Nigeria. The study area was mapped and lithological units and structural features were identified and studied. A total of twenty-seven (27) samples from five (5) wells (AMR 014, AMR 036, AMR 038, AMR 048, and AMR 049) of the study area were collected, prepared and subjected to geochemical analysis for both major and trace elements using EDX3600B X-ray fluorescence spectrometer. The analytical data were statistically computed using principal component factor analysis PCFA, statical package for social science SPSS, descriptive statistics DS, correlation matrix CM and were also adopted for various geochemical plots using Excel Microsoft office, geochemical data kid GCD Kid and Suffer software for geological map digitization, to determine the geochemical characteristics of the Lead-Zinc ore, the host rock and the environment of formation. The geology of the study area is strategically part of the Lower Benue Trough of Nigeria, it is made up of shale intruded by several small to medium sized mesocratic – melanocratic, phaneritic intrusives which are alkaline in nature with a slight variation in their mineralogical and textural characteristics. Structurally, the fractured zones or veins marked along the Enyigba and Ameka lodes could also be responsible for the mineralization of the Ameri Lead-Zinc. The Lead-Zinc in Ameri is associated with other gangue minerals such as marcasite, pyrite, quartz veins, carbonate materials, chalcopyrite, siderites, sphalerites and it shows that the Lead-Zinc mineralization in the study area is hosted by shales, which are probably parts of the slightly deformed cretaceous sedimentary rocks made up of essentially Albian shales and subordinate siltstones. Values of lead within this shear zone ranges from 0.06% - 64.58%, 0.02% - 64.35%, 0.01% - 0.14%, 0.03% - 0.11% for AMR 036, AMR 038, AMR 048, AMR 049 respectively, while Zn ranges in value from; 0.09% - 53.98%, 0.08% - 1.11%, 0.19% - 58.64%, 0.08% - 56.11%. The value of lead and zinc within the hanging wall are 0.06% and 0.08%, 0.03% and 0.06%, 0.04% and 0.12%, 0.04% and 0.13% for AMR 036, AMR 038, AMR 048, AMR 049 respectively. Paleo-redox condition of Low Cu/Zn ratios from 0.001-0.324, 0.001 – 0.307, 0.075-0.424, 0.001-0.309 and 0.001-0.321 for AMR 014, AMR 036, AMR 038, AMR 048, AMR 049 indicate more oxidizing conditions. This is confirmed by the Ni/Co ratio of 0.00-58.50, 0.00- 43.625, 0.00- 35.333, 0.00-1.704, 0.211- 1.472 for AMR 014, AMR 036, AMR 038, AMR 048, AMR 049 respectively mostly below the ratio indicated to be oxidic with little anoxic environmental affinity. The total Alkalis versus Silica plot from the intrusive revealed their basic to ultrabasic nature, as the bivariate plots of the analyzed samples shows positive and /or strong relationship between the trace elements in the Ameri lodes and their respective certified concentration values which is also an indicator that the elements are probably from same hydrothermal source with the Lead-Zinc of the study area.*

**KEY WORDS:** Ameri, geology, geochemistry, mineralization, paleo-redox and structure.

## INTRODUCTION

The geology of Nigeria is made up of three major litho-petrological components, namely, the Basement Complex, Younger Granites, and Sedimentary Basins. The Basement Complex, which is Precambrian in age, is made up of the Migmatite-Gneiss Complex, the Schist Belts, and the Older Granites. The Younger Granites comprise several Jurassic magmatic ring complexes centred around Jos and other parts of north-central Nigeria. They are structurally and petrologically distinct from the Older Granites. The Sedimentary Basins, containing sediment fill of Cretaceous to Tertiary ages, comprise the Niger Delta, the Benue Trough, the Chad Basin, the Sokoto Basin, the Mid-Niger (Bida/Nupe) Basin and the Dahomey Basin. The Benue Trough is a graben, representing the failed arm of a triple junction. The generated faults in the Trough range from major to small and micro types (Ofoegbu, 1985). The origin and subsequent evolution of the trough (occupied by the basin) remain controversial. Earlier workers (King, 1950; Carter *et al.*, 1963; Kennedy, 1965) felt that the trough was simply a fracture developed because of the tension set up by differential stresses during the break-up of Gondwanaland some 90 million years ago.

The basin is a narrow (80 – 150 km) linear basin which trends Northeast – Southwest (NE – SW) and extends from below the Niger delta to the southern limit of the Chad basin (Odebode, 2010). It is widely held to have originated as a tectonic trough whose origin was closely linked with the separation of African and South America during the Mesozoic (King, 1950; Cratchley & Jones, 1965). The basin has a 6,000-metre-thick Cretaceous sedimentary fill which is uniquely folded parallel to its axis. It also contains substantial economic deposits such as Lead-Zinc, coal, copper, barite (NGSA, 2009; Offodile, 1980). The Anambra Basin – Calabar Flank region is generally considered as an Upper Cretaceous – Lower Tertiary descendant of the Southern (Lower) Benue Trough. While it is widely accepted that the Benue Trough originated during the separation of Africa and South America in the Mesozoic, its precise origin and subsequent evolution remain controversial (King, 1962; Carter *et al.*, 1963; Burke *et al.*, 1970; Grant, 1971; Nwachukwu, 1972; Wright, 1968, 1981; Olade, 1976; Freeth, 1977; Benkheilil, 1982). The Trough, which is believed to have originated as a failed arm of an aulacogen at the time of the opening of the South Atlantic Ocean during the separation of the African plate from the South American plate (King, 1950; Kennedy, 1965, and Kogbe *et al.*, 1981), is partitioned into the Lower, Middle, and Upper regions. No concrete line of subdivision can be drawn to demarcate the individual portions, but major localities (towns/settlements) that constitute the depocentres of the different portions have been well documented (Petters, 1978; Nwajide, 1990; Idowu and Ekweozor, 1993; Obaje *et al.*, 1999 and Obaje, 2009), with Lead-zinc mineralization occurring in almost the entire 800km length. The structural features of the Benue Trough are represented mostly by folds produced during the Cenomanian (Nwachukwu, 1972) and Santonian (Orajaka 1965, Olade, 1976) tectonic deformations. In the Lower Benue an intense compressive folding produced the major Abakaliki anticlinorium and minor anticlines and synclines (Burke *et al.*, 1970).

This paper examines the occurrence of Pb-Zn and the relationship between the Ore and host lithologies around Ameri areas of Southeastern Nigeria with emphasis on the structural control,

geochemistry of both the host rock, the ore, and their environment of formation. The area of study has generated a lot of interests because of medium scale mining in the adjoining communities which share similar geological information within the Middle and Lower Benue Trough and the need to expand search for valuable mineral of economic interest, hence, Ameri become a prime geological target for Pb-Zn exploration and exploitation.

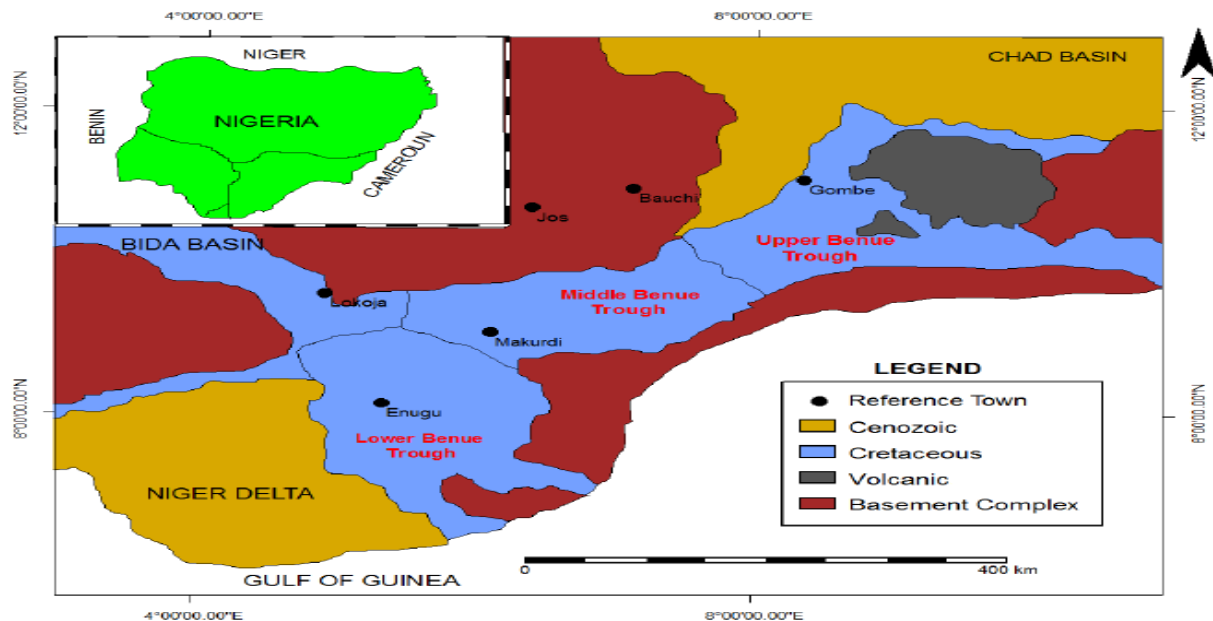


Figure 1: Geological map of Nigeria showing Upper, Middle and Lower Benue Trough, and other inland basins (Obaje *et al.*, 1999)

### Geology of the Study Area

The geology of the study area is made up of shale intruded by several small to medium sized mesocratic –melanocratic, phaneritic intrusive which are alkaline in nature with a slight variation in their mineralogical and textural characteristics Figure 2 Parts of the Ebonyi State Lead-Zinc localized in Ameri, and its environs are along the Northeast-Southwest trending belt of slightly deformed volcanic and sedimentary Cretaceous sequences (Albian Asu River Group) which is about 500 m thick, and they occur in the form of veins and veinlets associated with the host rock (Shales).

The Lead-Zinc mineralization in Ameri is hosted by Shales, which are probably parts of the slightly deformed cretaceous sedimentary rocks made up of essentially Albian shales and subordinate siltstones (Figure 2). The fractured zones or veins marked along the Enyigba and Ameka lodes could also be responsible for the mineralization of the Ameri Lead – Zinc. The Lead-Zinc in Ameri is associated with other gangue minerals such as marcasite, pyrite, quartz veins, carbonate materials, chalcopyrite, siderites, sphalerites etc. (Figure3).

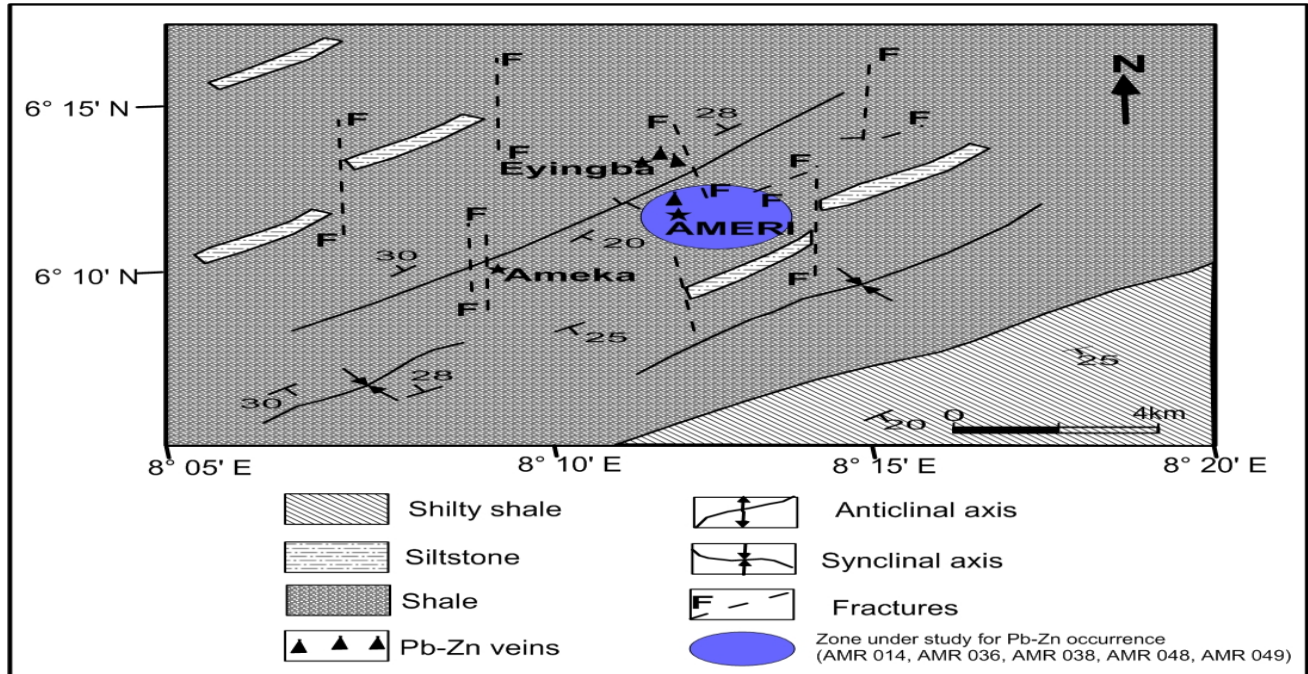


Figure 2: Geological Map of the Study Area

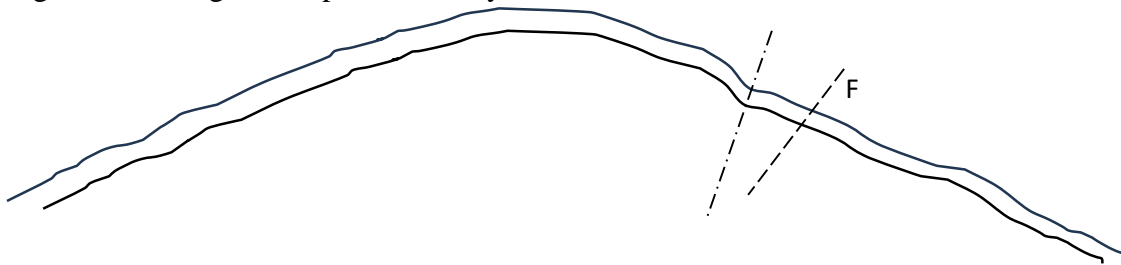


Figure 3. Cross section of the anticline and the fractures of the Pb-Zn mineralization in the study area

The mineralization evolution in Ameri and its environs is like the Ishiagu ore reports of Akande & Mucke (1989) and Ogundipe & Obasi (2016) based on their geologic settings and structural characteristics. Ore deposit consist of massive sphalerite, galena, chalcopyrite, marcasite, siderite, calcite, and quartz veins in descending abundance and proposed the three stages of event in the evolution of the Lead –Zinc deposit to be.

- i. Pre-ore fracturing and brecciation of the Albian shales accompanied by the precipitation of pyrite, siderite, and quartz.
- ii. Ore stage formation of sphalerite, galena, and copper bearing minerals (chalcopyrite).
- iii. Final deposition of octahedral galena, sphalerite, and marcasite in the hanging walls of the veins.

Both ore and gangue minerals occur in successive, symmetrical layers along vertical and/or steeply dipping fractures which often have parallel walls with the host rock indicating fissure filling mode of occurrence.

## **MATERIALS AND METHOD**

A total of twenty-seven (27) representative core samples, from Five (5) wells (AMR 014, AMR 036, AMR 038, AMR 048, and AMR 049) were collected for this study using core drilling machine, GPS, compass, hammer, sampling bags, marker pen, field notebook, measuring tape, hydrochloric acid (HCl), field material. The samples were lithologically described on depth-by-depth basis, paying close attention to variations in lithology, texture, thickness, sedimentary structures, and dominant and accessory minerals. Based on the core description, lithologic logs were generated for the five wells under investigation with their descriptions given accordingly. The samples were firstly, air-dried and ground into fine powder to yield an acceptable number of particles of each component of the heterogeneous material. The samples were sieved through a sieve of 60 urn size. The prepared samples were then analyzed using EDX3600B X-ray fluorescence spectrometer which applies XRF technology to conduct fast and accurate analysis of complex composition. The system detects elements between Magnesium (Mg,  $z=12$ ) and Uranium (U,  $z=92$ ) with high resolution and speed.

The geochemical data was subjected to multivariate statistical analysis using SPSS (PASW 18) for Windows using methods described by Field (2009). Descriptive statistics (DS), correlation matrix (CM), principal component factor analysis (PCFA) and One-way repeat-measures ANOVA were performed on the data. While carrying out descriptive statistics (DS), correlation matrix (CM) and PCFA. For the repeat-measures ANOVA, a correction for data sphericity was carried out using Bonferroni method. Descriptive statistics provide a summary of the data in terms of its statistical parameters of minimum and maximum, and mean. Correlation matrix was used to obtain the Pearson relationship between the elements. The PCFA was performed to identify possible sources and fate of the various elements. Multi- element graphs of the data were plotted using the chart option in Microsoft Office Excel 2007.

## **RESULT AND DISCUSSION**

The mineralization evolution in Ameri and its environs is like that of the Ishiagu ore reports of Akande & Mucke (1989) and Ogundipe & Obasi (2016) based on their geologic settings and structural characteristics. Ore deposit consist of massive sphalerite, galena, chalcopyrite, marcasite, siderite, calcite, and quartz veins in descending abundance and proposed the three stages of event in the evolution of the Lead –Zinc deposit to be.

- i. Pre ore fracturing and brecciation of the Albian shales accompanied by the precipitation of pyrite, siderite, and quartz.
- ii. Ore stage formation of sphalerite, galena, and copper bearing minerals (chalcopyrite).



- iii. Final deposition of octahedral galena, sphalerite, and marcasite in the hanging walls of the veins.

Both ore and gangue minerals occur in successive, symmetrical layers along vertical and/or steeply dipping fractures which often have parallel walls with the host rock indicating fissure filling mode of occurrence.

### **Structural geology of the Study Area**

Ameri is one of the localities in Enyigba district that is sufficiently mineralized. Its minerals are mainly of high-grade sphalerite mineralization. Fractures were not observed/identified at the exposed outcrop but were seen controlling the mineralization as exposed by the lithology section (Figure 5 - 9), which also reveals fault and folds. The bed strikes N20°E - N57°E having a dip direction of South-East as one of the limbs of the anticlinal fold (Figure 2) with dip ranging from 9° to 31°. The fracture that controls the mineralization has trends N-S with a probably strike length of 950 m with 5.5 m width. The core log section (Figure 5 - 9) shows that the outcrop was fractured, moderately-steeply folded, and faulted. Ameri lode host more sphalerite than galena, but of a low grade than Enyigba.

The deposits in Ameri were formed epigenetically through the crystallization of hydrothermal solutions and are localized within the fractures. From the detailed field mapping, the identified structures that control the mineralization are fold, fault, and joint/fractures in which the fractures predominate. The veins appeared to be continuous extension of the Enyigba mineralization, steeply dipping N-S near vertical fault cutting across the anticline structures.

### **Structural Interpretation**

The structures dominating the area are faults, folds, and fractures. These deformative structures observed was probably due to tectonic events which occurred during the Santonian-Coniacian's times, at which the Albian and Turonian sediments were deformed along north-westerly trending axes, producing numerous gently folds. Fractures, fault, and folds are the structural features observed in the study (Table 1).



Plate 1: Showing ore vein and surrounding rock exposed by Artisanal mined Pb-Zn vein cutting across the intrusive



Plate 2: Showing



Plate 3: Showing the Pit geometry around Project area



Plate 4: Showing

### **Fold**

The fold occurred because of compressional forces acting at the sediment. From Figure 2, series of fold occurrence at the study area across the sediment with syncline and anticline. However, the sediment is highly folded. The mineralization was gently to steeply folded, and it is obviously folded at the eastern part of the section throwing the deposit up to 50 m close to the surface. This indicates series of tectonic events which occurred within the Santonian-Coniacian times.

### **Fault**

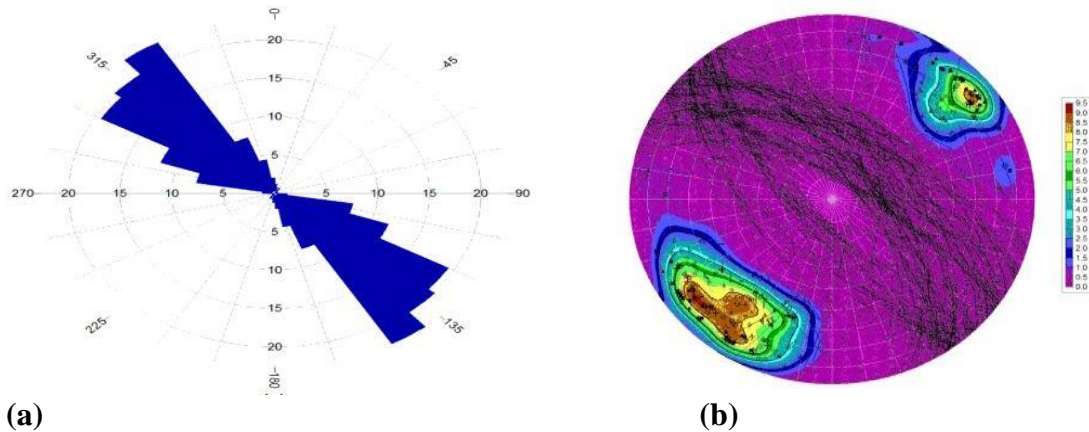
Fault was also observed in the study area. Ameri core logged section shows the presence of fault by the discontinuity of the mineral of interest. Orajaka (1975) commented that the anticlinal axis of the shale body passes up to Ameka village (Figure 2), that this axis has been evidently displaced at Ameka about the North shaft and Ameka lode of the ore deposit. The fault could occur because of the movement along the open fracture.

**Fractures**

Fracture is the major structural feature that controls the mineralization. The fractures trend NW-SE and N-S directions (Table 1). The fractures make the deposit to be an open space filling. At Ameri, the main fractures that controls the mineralization trends N-S directions with a strike length of 950 m and width of 5.5 m. It hosts more Zinc deposit than Lead, but Zinc is of lower grades compared to Enyigba deposit.

N64°W,S57°E,S52°E,S58°E,N29°W,N4°W,S65°E,S10°E,S80°E,S52°E,N45°W,S52°E,N69°W ,N78°W,N32°W,N60°W,S52°EN19°W,N24°W,S52°E,N59°W,N21°W,S53°EN19°W,N40°W,S53°E,N49°W,N70°W,S50°E,N69°W,N46°W,N39°W,N70°W,N35°W	6	5
N15°W,N25°W,N24°W,N42°W,N32°W,N45°W,N46°W,S56°E,N74°W,N72°W,S48°E,N74°W,N19°W,S30°EN37°W,N28°W,S80°E,S76°E,S35°E,S26°ES65°E,S51°E,N38°W,S10°E,S15°E,N28°W,N24°W,N29°W,S51°E,N21°W,N33°W,S80°E,S43°E,S22°E,N15°W	15	2
S55°E,N24°E,N23°EN26°E,N62°E,N55°E,N56°E,N66°E,N64°EN68°E,N15°E,N55°E,S38°E,S40°E,S45°E,S48°E,S50°E,S53°E,S46°E,S47°E,S49°E,S45°E,S55°E,N45°W,S53E	28	3
S50°E,S55°E,S56°E,S55°E,N54°W,S47°E,S49°E,S55°ES42°E,N65°W,N35°W,N45°W,N16°W,S55°EN55°W,N23°W,S55°E,N52°W,N25°W,N23°W,N22°W,N20°W,N34W	54	
N55°W,S45°E,N54°W,N55°W,S55E,N16°W,N23°W,N25°W,N22°W,N17°W,N48°W,N53°W, N9°W,N31°WN20°W,N33°W,N34°W,N34°W,S25°E,S45°E,S60°ES36°E,S38°E,S34°E,S53°E, S52°E,S45°E,S52°E,S42°E,N41°W,N40°W,N35°W,S45°E,N42°W,N4	52	
N55°W,N53°W,N56°W,N59°W,N60°W,N77°W,N83°W,N78°WN34°W,N32°W,N31°W,N36°W,N37°W,N35°W,N34°W,N40°W,N38°W,N34°W,N36°W,N35°W,N15°W,N14°W,N13°W,N31°W,N30°W,N36°W,N38°W,N32°W,N31°WN35°W,N16°W	1	





(a) (b)  
Figure 4: Diagram showing the trend of fractures at Ameri. (a) Rose diagram and (b) Stereo net indicates that the fracture dips NE-SW.

#### Table 1: Frequency of Ameri lodes Fractural trends

##### Lithology of the Study Area

The samples under investigation are predominantly shales ranging from coarse to fine grained size texture. Sample cores collected - vary in colour from black to greyish black, except the reddish brown lateritic top layer probably from a weathered iron rich material associated with clays which often ranges from 2m – 8m in most wells. Greyish brown to greyish black broken calcareous shale is often observed from 10 – 60m. The shale is fissile, thinly laminated and highly fractured and weathered within these rock units. Similarly, greyish black to black calcareous shales are observed from 70m -120m and beyond. The rock units are thinly laminated and fractured, hosting the mineralization, very hard, compacted and indurated fissile shale. Also associated with the shales are veins of quartz, and or carbonate materials, stringers and fragments of pyrite, and chalcopryrite, fragments of siderite materials. Detailed lithological description of the collected core samples (A –E) are shown below (Plates1-4 and Figures 5- 9).



Core-log	Depths (m)	Lithologies	Description
	0 - 2	Top lateritic soil	Layer characterized by coarse grained reddish brown soil material (probably from weathered iron rich material associated with clay material)
	3 - 5	Shale	Characterized by fine grained brownish broken shale associated with fragmented and powdery shale
	6 - 8	Shale	Characterized by fine grained, black broken shale, associated with tiny veins of carbonate materials
	9 - 20	Shale	Characterized by fine grained, black broken shale, associated with tiny veins of carbonate materials
	21 - 23	Shale	Characterized by fine grained, black broken shale, associated with thick vein (about 1m) of carbonate materials
	24 - 59	Shale	Characterized by fine grained, black highly broken shale, associated with thin vein of carbonate materials
	60 - 62	Shale	Characterized by fine grained, black fairly compacted shale
	63 - 65	Shale	Characterized by fine grained, black fairly fragmented shale
	66 - 68	Shale	Characterized by fine grained, black fairly compacted shale, associated with fragmented quartz veins and carbonate materials
	69 - 128	Shale	Characterized by fine grained, black broken shale, associated with thin vein of carbonate materials
	129 - 131	Shale	Characterized by fine grained, black highly fragmented shale, associated with veins of carbonate materials, quartz and minor stringers and fragmented pyrite

Figure 5 Lithological description of Core sample A-AMR 014








Core-log	Depths (m)	Lithologies	Description
	0 - 4	Top lateritic soil	Layer characterized by fine to coarse grained reddish brown soil material (probably from weathered iron rich material associated with clay material)
	5 - 8	Lateritic soil	Characterized by fine to coarse grained reddish (about 50cm) to greyish soil material (highly weathered shale)
	9 - 17	Shale	Characterized by fine grained, greyish broken shale, associated with thin and thick veins of carbonate materials
	18 - 20	Shale	Characterized by fine grained, greyish broken shale, associated with thicker veins of carbonate materials. Specks of chalcopyrite was also observed
	21 - 38	Shale	Characterized by fine grained, greyish broken shale, associated with veins of carbonate materials
	39 - 40	Shale	Characterized by fine grained, greyish broken shale, associated with thick veins of quartz and carbonate materials
	41 - 43	Shale	Characterized by fine grained, greyish broken shale, associated with fragments of quartz and carbonate materials
	44 - 65	Shale	Characterized by fine grained, grayish-black broken shale
	66 - 68	Shale	Characterized by fine grained, greyish black shale, associated with veins of quartz and carbonate materials
	69 - 71	Shale	Characterized by fine grained, greyish black fairly compacted shale, associated with thin veins of carbonate materials
	72 - 74	Shale	Characterized by fine grained, greyish broken shale, associated with thick veins of quartz and carbonate materials, veins of siderite, and clusters of pyrite
	75 - 77	Shale	Characterized by fine grained, greyish broken shale, associated with thick veins of carbonate materials and thin veins of siderite materials
	78 - 80	Shale	Characterized by fine grained, greyish broken shale, associated with thick veins of carbonate materials
	81 - 83	Shale	Characterized by fine grained, greyish broken shale, associated with thin veins of carbonate materials and thin and thick veins of siderite materials, stringers of pyrite and minor blebs galena
	84 - 86	Shale	Characterized by fine grained, greyish broken shale, associated with thin and thick veins of carbonate materials, quartz, thick sheared veins of siderite, minor blebs and stringers of sphalerite
87- 90	Shale	Characterized by fine grained, greyish broken shale, associated with thin and thick veins of carbonate materials, quartz, thick sheared veins of siderite, minor blebs and stringers of sphalerite, galena	

Figure 6: Lithological description of Core sample B-AMR 036



Core-log	Depths (m)	Lithologies	Description
	0 - 4	Top lateritic soil	Layer characterized by fine to coarse grained reddish brown soil material (probably from weathered iron rich material associated with clay material)
	5 - 7	Lateritic soil	Characterized by fine to coarse grained reddish (about 95cm) to greyish soil material (highly weathered shale)
	8 - 10	Shale	Characterized by fine grained, greyish broken shale
	11 - 15	Shale	Characterized by fine grained, greyish broken shale
	16 - 19	Shale	Characterized by fine grained, greyish broken shale, associated with large fragmented carbonate materials
	20 - 31	Shale	Characterized by fine grained, greyish broken shale
	32 - 33	Shale	Characterized by fine grained, greyish broken shale, associated with fragments of carbonate materials
	34 - 38	Shale	Characterized by fine grained, greyish-black broken shale
	39 - 41	Shale	Characterized by fine grained, greyish black shale, associated with veins of carbonate materials
	42 - 47	Shale	Characterized by fine grained, greyish-black broken shale
	48 - 50	Shale	Characterized by fine grained, greyish broken shale, associated with thick veins of carbonate materials, siderite and specks of pyrite
	51 - 53	Shale	Characterized by fine grained, greyish broken shale, associated with thick veins of carbonate materials, thin veins of siderite materials and mixed composition of well formed crystal of chalcopyrite
	54 - 56	Shale	Characterized by fine grained, greyish compacted shale, associated with thick veins of carbonate materials
	57 - 59	Shale	Characterized by fine grained, greyish compacted shale, associated with thick veins of carbonate materials and thin veins of siderite
	60 - 62	Shale	Characterized by fine grained, greyish compacted shale, associated with thick veins of carbonate materials and thin veins of siderite
	63 - 65	Shale	Characterized by fine grained, greyish compacted shale, associated with thick and thin veins of carbonate materials
	66 - 68	Shale	Characterized by fine grained, greyish compacted shale, associated with thin veins of carbonate materials
	69 - 71	Shale	Characterized by fine grained, greyish compacted shale, associated with veins of carbonate materials
	72 - 74	Shale	Characterized by fine grained, greyish compacted shale, associated with thin veins of carbonate materials
	75 - 77	Shale	Characterized by fine grained, greyish compacted shale, associated with siderite materials and thicker veins of carbonate materials
78 - 80	Shale	Characterized by fine grained, greyish broken shale	
81 - 83	Shale	Characterized by fine grained, greyish broken shale, associated with thick veins of carbonate materials and siderite	
84 - 86	Shale	Characterized by fine grained, greyish broken shale, associated with thin veins of carbonate materials	
87 - 89	Shale	Characterized by fine grained, greyish broken shale, with compositional banding of 45° core angle	





90 - 92	Shale	Characterized by fine grained, greyish broken shale, associated with quartz/ siderite material, thick veins of carbonate and thin layers of compositional banding of 35° core angle
93 - 95	Shale	Characterized by fine grained, greyish broken shale, associated with thin layers of compositional banding and thin vein of carbonate materials
96 - 98	Shale	Characterized by fine grained, greyish broken shale, associated with thin veins of carbonate and thin layers of compositional banding of 30° core angle
99 - 101	Shale	Characterized by fine grained, greyish broken shale, associated with thin veins of carbonate and barite materials, stringers of sphalerite, patches of galena and thicker vein of siderite
102 - 104	Shale	Characterized by fine grained, greyish broken shale, associated with, patches of galena, wide patches of sphalerite and specks of pyrite
105 - 107	Shear zone	Characterized by fine grained, greyish broken shale, associated with thin veins of quartz/carbonate materials, thick and thin veins of siderite and pyrite crystals
108 - 110	Shear zone	Characterized by fine grained, greyish broken shale, associated with thin and thick veins of quartz/carbonate materials, thick and thin veins of siderite and thick and wide patches of sphalerite
111 - 113	Shear zone	Characterized by fine grained, greyish broken shale, associated with thin and thick veins of quartz, thick and thin veins of siderite and thick and wide patches galena, minor and wide patches of sphalerite
114 - 116	Shear zone	Characterized by fine grained, greyish broken shale, associated with massive and thick sphalerite vein and wide patches of siderite and veins of siderite
117 - 119	Shear zone	Characterized by fine grained, greyish broken shale, associated with thick veins of siderite, stringers of sphalerite, veins of quartz, patches of chalcopryite and pyrite and veins of galena
120 - 122	Shear zone	Characterized by fine grained, greyish broken shale, associated with thick veins of quartz, thick veins of galena, stringers and wide patches of sphalerite, clusters of pyrite crystals and well formed quartz

Figure 7: Lithological description of Core sample C-AMR 038







Core-log	Depths (m)	Lithologies	Description
	0 - 2	Top lateritic soil	Layer characterized by fine brown lateritic soil material (probably from weathered iron rich material associated with clay material)
	3 - 5	Lateritic soil	Layer characterized by fine brown lateritic soil material (probably from weathered iron rich material associated with clay material)
	6 - 8	Lateritic soil + Shale	Characterized by fine grained, brown and fragmented shale
	9 - 11	Shale	Characterized by fine grained, greyish black shale, associated with fragmented carbonate materials
	12 - 14	Shale	Characterized by fine grained, greyish black shale, associated with fragmented carbonate materials
	15 - 17	Shale	Characterized by fine grained, greyish black shale, associated with thick veins of carbonate materials, quartz and minor patches of siderite and stringers of pyrite
	18 - 20	Shale	Characterized by fine grained, greyish black shale, associated with thick veins of carbonate materials
	21 - 23	Shale	Characterized by fine grained, greyish black shale, associated with thick veins of carbonate materials
	24 - 26	Shale	Characterized by fine grained, greyish black shale, associated with thick veins of siderite, fragments and thick veins of carbonate materials,
	27 - 29	Shale	Characterized by fine grained, black broken shale, associated with thin and fragments of siderite
	30 - 32	Shale	Characterized by fine grained, greyish black broken shale, associated with thick and thin veins of carbonate and siderite
	33 - 35	Shale	Characterized by fine grained, greyish black broken shale, associated with thick and thin veins of carbonate materials
	36 - 38	Shale	Characterized by fine grained, greyish black broken shale, associated with thick and thin veins of carbonate materials
	39 - 41	Shale	Characterized by fine grained, greyish black broken shale, associated with fragments of siderite
	42 - 44	Shale	Characterized by fine grained, greyish black broken shale, associated with fragments of siderite
	45 - 47	Shale	Characterized by fine grained, greyish black broken shale
	48 - 50	Shale	Characterized by fine grained, greyish black broken shale, associated with fragments of carbonate and siderite
	51 - 53	Shale	Characterized by fine grained, greyish black broken shale, associated with fragments of carbonate materials
	54 - 56	Shale	Characterized by fine grained, greyish black broken shale, associated with fragments of carbonate materials
	57 - 59	Shale	Characterized by fine grained, greyish black broken shale, associated with patches of siderite
60 - 62	Shale	Shale	Characterized by fine grained, greyish black broken shale, associated with clusters of pyrite, thick veins of carbonate materials and siderite, disseminated galena crystals
	63 - 65	Shale	Characterized by fine grained, greyish black broken shale, associated with thick veins of carbonate materials
	66 - 68	Shale	Characterized by fine grained, greyish black broken shale, associated with thin and thick veins of carbonate materials
	69 - 71	Shale	Characterized by fine grained, greyish black broken shale, associated with thin and thick veins of siderite and carbonate materials
	72 - 74	Shear zone	Characterized by fine grained, greyish black broken shale, associated with thick veins of siderite, thin veins of carbonate materials, thick and minor patches of sphalerite

Figure.8: Lithological description of Core sample C-AMR 038



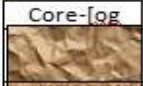


Core-log	Depths (m)	Lithologies	Description
	0 - 2	Top lateritic soil	Layer characterized by fine brown lateritic soil material
	3 - 5	Lateritic soil	Layer characterized by fine brown lateritic soil material
	6 - 8	Shale	Characterized by fine grained, greyish black and fragmented shale
	9 - 11	Shale	Characterized by fine grained, greyish black shale, associated with thin veins carbonate materials
	12 - 14	Shale	Characterized by fine grained, greyish black shale, associated with thin veins of siderite and carbonate materials
	15 - 17	Shale	Characterized by fine grained, greyish black shale, associated with thin veins of carbonate materials.
	18 - 20	Shale	Characterized by fine grained, greyish black shale, associated with thick and thin veins of carbonate materials
	21 - 23	Shale	Characterized by fine grained, greyish black shale, associated with thin veins of carbonate materials
	24 - 26	Shale	Characterized by fine grained, greyish black shale, associated with thin veins of carbonate materials
	27 - 47	Shale	Characterized by fine grained, black broken shale
	48 - 50	Shale	Characterized by fine grained, greyish black broken shale, associated thin veins of carbonate and siderite
	51 - 53	Shale	Characterized by fine grained, black broken shale
	54 - 56	Shale	Characterized by fine grained, black fragmented and broken shale
	57 - 59	Shale	Characterized by fine grained, greyish black broken shale, associated with thin veins of siderite and carbonate materials
	60 - 62	Shale	Characterized by fine grained, greyish black broken shale, associated with thin veins of carbonate materials
	63 - 65	Shale	Characterized by fine grained, greyish black broken shale associated with thick veins of siderite materials
	66 - 68	Shale	Characterized by fine grained, greyish black broken shale, associated with minor veins of carbonate and siderite, well formed quartz crystals in association with specks of pyrite crystals
	69 - 71	Shale	Characterized by fine grained, greyish black broken shale, associated with thicker veins of siderite and fragments of quartz materials
	72 - 74	Shale	Characterized by fine grained, greyish black broken shale, associated with thin veins of carbonate materials and thick veins of siderite
75 - 77	Shale	Characterized by fine grained, greyish black broken shale, associated with thin and thick veins of carbonate and siderite materials and thin veins of quartz	
78 - 80	Shear zone	Characterized by fine grained, greyish black broken shale, associated with veins of quartz, stringers and fragmented fresh pyrite crystals, veins of siderite and massive mineralization of sphalerite, fresh pyrite crystals	
81 - 83	Shear zone	Characterized by fine grained, greyish black broken shale, associated with thick veins of siderite, well formed quartz crystals, and fragmented pyrites, thick and wide patches of sphalerite	

Figure 9: Lithological description of Core sample E-AMR 049.

### Geochemistry of the Study Area

The results of the elemental composition of the analyzed samples are shown in Tables 2–6. Lead-zinc in the Ameri lode shows a significant concentration within the shear zone, as against the hanging and footwall samples (Tables.2 – 6). The shear zone often contains significant amount of lead, and or zinc. Values of lead within this shear zone ranges from 0.06% - 64.58%, 0.02% - 64.35%, 0.01% – 0.14%, 0.03% - 0.11% for AMR 036, AMR 038, AMR 048, AMR 049

respectively, while zinc ranges in value from; 0.09% - 53.98%, 0.08% - 1.11%, 0.19% - 58.64%, 0.08% - 56.11%. The value of lead and zinc within the hanging wall are 0.06% and 0.08%, 0.03% and 0.06%, 0.04% and 0.12%, 0.04% and 0.13% for AMR 036, AMR 038, AMR 048, AMR 049 respectively. Lead and zinc concentrations in the footwall varies from 0.05% - 0.12% and 0.16% - 0.28% in AMR 038 while in AMR 048, the values are 0.14% and 0.05% for lead and zinc respectively. However, AMR 014 which exhibit no shear zone has values ranging from 0.00% - 66.99% and 0.10% - 57.61% for lead and zinc respectively (Tables 2 –6).

Table 2: Elemental compositions of samples from well AMR 014

Sample No.	AMR 014 A	AMR 014 B	AMR 014 C	AMR 014 D
Elements	Content (%)	Content (%)	Content (%)	Content (%)
Mg	0.0000	0.0000	0.0000	0.0000
Al	1.1682	1.2165	0.6357	1.0012
Si	1.3236	1.2384	0.4573	1.3382
P	0.2209	0.2230	0.2174	0.1938
S	21.2753	17.3028	19.2628	15.7735
K	0.0056	0.0000	0.0000	0.0000
Ca	0.0202	2.6981	0.0226	0.1277
Ti	0.0000	0.0000	0.0000	0.0000
V	0.0043	0.0083	0.0035	0.0054
Cr	0.0005	0.0220	0.0000	0.0062
Mn	0.0007	1.9811	0.0029	0.4171
Co	0.0006	0.0000	0.0423	0.0133
Fe	0.2141	25.4344	1.9010	9.2323
Ni	0.0351	0.0458	0.0588	0.0546
Cu	0.0319	0.0252	0.0355	0.0343
Zn	0.0984	25.2211	57.6126	48.0710
As	2.7717	0.0018	0.0000	0.0000
Pb	66.9896	0.0663	0.0000	0.0173
W	0.0000	17.5973	36.8378	31.9183
Au	3.0634	0.0000	0.0046	0.0000
Ag	0.0000	0.0000	0.0003	0.0000
Rb	0.0000	0.0004	0.0000	0.0000
Nb	0.0000	0.0000	0.0000	0.0000
Mo	0.0385	0.0461	0.0000	0.0000
Cd	0.0050	0.0006	0.0011	0.0006
Sn	0.7689	0.0774	0.0961	0.0769
Sb	0.0336	0.0617	0.0812	0.0672



Table 3: Elemental compositions of samples from well AMR 036

Sample No.	AMR 036 A	AMR 036 B	AMR 036 C	AMR 036 D	AMR 036 E	AMR 036 F	AMR 036 G	AMR 036 H
Element	Content (%)	Content (%)	Content (%)	Content (%)	Content (%)	Content (%)	Content (%)	Content (%)
Mg	0.0000	0.7912	0.0000	0.0000	0.0000	0.0000	0.0000	0.0000
Al	5.4227	0.4481	0.8104	0.8412	0.7721	0.9296	1.2736	8.7419
Si	15.2185	0.5461	0.7163	0.4693	0.5648	4.2774	3.3290	28.4494
P	0.2990	0.0336	0.2260	0.2340	0.2373	0.1957	0.2037	0.3332
S	2.0388	0.7381	20.6923	20.7971	22.9489	17.7070	16.6547	15.4153
K	1.1791	0.0000	0.0000	0.0146	0.0000	0.0087	0.0000	2.6086
Ca	38.0699	3.2004	0.0147	0.0135	0.0136	0.0334	0.1072	4.7888
Ti	0.0000	0.0000	0.0000	0.0000	0.0000	0.0000	0.0000	0.2535
V	0.0087	0.0195	0.0038	0.0036	0.0044	0.0031	0.0056	0.0177
Cr	0.0051	0.0521	0.0000	0.0017	0.0000	0.0000	0.0052	0.0073
Mn	0.1653	5.0531	0.0051	0.0046	0.0015	0.0032	0.2596	0.0538
Co	0.0463	0.0000	0.0182	0.0443	0.0008	0.0161	0.0244	0.1441
Fe	6.6918	59.4660	1.1130	3.5587	0.1177	1.1009	6.9786	9.3453
Ni	0.0273	0.0468	0.0404	0.0602	0.0349	0.0431	0.0550	0.0458
Cu	0.0178	0.0155	0.0322	0.0376	0.0278	0.0338	0.0344	0.0271
Zn	0.0764	0.1129	20.5245	53.9755	0.0905	17.9594	47.1557	0.1230
As	0.0089	0.0041	1.5438	0.0101	2.7620	1.6244	0.0252	0.0230
Pb	0.0581	0.1855	31.3094	0.0628	64.5870	34.1392	0.1181	0.1028
W	0.0455	0.0215	14.5758	35.2429	0.0000	12.9931	31.0510	0.0876
Au	0.0226	0.0000	1.8661	0.0068	3.2248	1.8701	0.0105	0.0112
Ag	0.0001	0.0000	0.0010	0.0009	0.0000	0.0017	0.0000	0.0000
Rb	0.0053	0.0036	0.0000	0.0000	0.0000	0.0000	0.0011	0.0678
Nb	0.0033	0.0000	0.0000	0.0000	0.0000	0.0000	0.0000	0.0054
Mo	0.2391	0.0717	0.0100	0.0000	0.0284	0.0291	0.0000	0.2190
Cd	0.0000	0.0000	0.0022	0.0014	0.0050	0.0020	0.0011	0.0000
Sn	0.4429	0.1377	0.2890	0.0810	0.7625	0.2837	0.0974	0.7186
Sb	0.3987	0.0867	0.0446	0.0711	0.0347	0.0606	0.0987	0.6800

Table 4: Elemental compositions of samples from well AMR 038

<b>Sample No.</b>	<b>AMR 038 A</b>	<b>AMR 038 B</b>	<b>AMR 038 C</b>	<b>AMR 038 D</b>	<b>AMR 038 E</b>	<b>AMR 038 F</b>
Elements	Content (%)	Content (%)	Content (%)	Content (%)	Content (%)	Content (%)
Mg	1.3880	0.0000	0.0000	0.0000	0.0000	0.0000
Al	3.7508	7.1416	1.0704	0.9549	7.4254	10.7551
Si	9.3787	58.1127	2.0040	0.7959	27.3167	30.1054
P	0.2447	0.2236	0.1787	0.2388	0.2307	0.2345
S	2.9821	0.8104	16.1814	23.4715	8.1106	5.3263
K	0.6729	1.9636	0.0543	0.0004	2.5498	3.5346
Ca	32.6078	0.0604	0.2563	0.0310	3.2208	0.4045
Ti	0.0000	0.0581	0.0000	0.0000	0.0613	0.4344
V	0.0181	0.0155	0.0085	0.0046	0.0138	0.0184
Cr	0.0126	0.0019	0.0165	0.0000	0.0163	0.0187
Mn	0.8515	0.0070	1.3415	0.0014	1.5251	0.0588
Co	0.2040	0.0150	0.0000	0.0009	0.0361	0.2854
Fe	16.7802	2.5452	17.8579	0.1440	20.5726	15.0594
Ni	0.0246	0.0471	0.0374	0.0318	0.0353	0.0510
Cu	0.0157	0.0340	0.0246	0.0302	0.0211	0.0294
Zn	0.0645	0.1133	0.0580	0.0883	0.2803	0.1552
As	0.0005	0.0017	1.8102	2.7424	0.0056	0.0263
Pb	0.0347	0.0274	40.2911	64.3521	0.0495	0.1248
W	0.0000	0.0746	0.0000	0.0000	0.6386	0.1354
Au	0.0000	0.0000	1.9755	3.1995	0.0000	0.0000
Ag	0.0000	0.0000	0.0000	0.0000	0.0009	0.0000
Rb	0.0073	0.0654	0.0000	0.0000	0.0502	0.0693
Nb	0.0033	0.0065	0.0000	0.0000	0.0000	0.0081
Mo	0.2226	0.2174	0.0157	0.0265	0.2342	0.2135
Cd	0.0000	0.0002	0.0016	0.0051	0.0000	0.0000
Sn	0.3621	0.9495	0.3040	0.7959	0.3931	0.6698
Sb	0.3239	0.8918	0.0490	0.0322	0.3839	0.6130

Table 5: Elemental compositions of samples from well AMR 048

<b>Sample No.</b>	<b>AMR 048 A</b>	<b>AMR 048 B</b>	<b>AMR 048 C</b>	<b>AMR 048 D</b>
Elements	Content (%)	Content (%)	Content (%)	Content (%)
Mg	0.0000	0.1878	0.0000	0.9313
Al	5.3938	1.7453	0.7392	0.4358
Si	14.7797	5.2328	0.5881	0.4499
P	0.3799	0.1098	0.1981	0.0347
S	13.1053	3.6035	18.0958	0.4900
K	1.5784	0.0000	0.0163	0.0000
Ca	29.8149	3.2988	0.0358	3.0938
Ti	0.0159	0.0000	0.0000	0.0000
V	0.0076	0.0145	0.0033	0.0195
Cr	0.0073	0.0451	0.0000	0.0532
Mn	0.1728	4.3103	0.0248	5.4494
Co	0.0444	0.0000	0.0355	0.0000
Fe	6.8962	50.2668	2.0797	59.5313
Ni	0.0321	0.0366	0.0605	0.0446
Cu	0.0204	0.0147	0.0345	0.0171
Zn	0.1271	0.1909	58.6379	0.0553
As	0.0039	0.0101	0.0000	0.0000
Pb	0.0402	0.1469	0.0091	0.1494
W	0.1090	0.2059	37.9194	0.0187
Au	0.0255	0.0000	0.0000	0.0000
Ag	0.0000	0.0005	0.0000	0.0005
Rb	0.0140	0.0043	0.0000	0.0039
Nb	0.0060	0.0000	0.0000	0.0000
Mo	0.2388	0.1744	0.0000	0.0946
Cd	0.0000	0.0000	0.0006	0.0000
Sn	0.4236	0.1637	0.0988	0.1254
Sb	0.4268	0.1157	0.0698	0.0963

Table 6:

Elemental compositions of samples from well AMR 049

<b>Sample No.</b>	<b>AMR 049 A</b>	<b>AMR 049 B</b>	<b>AMR 049 C</b>	<b>AMR 049 D</b>	<b>AMR 049 E</b>
Elements	Content (%)	Content (%)	Content (%)	Content (%)	Content (%)
Mg	0.0000	0.0000	0.0000	0.0000	0.0000

## Publication of the European Centre for Research Training and Development -UK

Al	6.1248	1.2637	8.4780	5.4196	6.8267
Si	20.0304	1.0584	22.1619	47.5939	18.5750
P	0.3527	0.2084	0.2344	0.3082	0.2767
S	1.4996	18.7803	9.0193	8.0409	13.5236
K	1.9378	0.0625	3.3441	1.2344	2.3843
Ca	33.5810	0.0235	1.8616	0.6783	2.3441
Ti	0.0000	0.0000	0.1902	0.0000	0.2250
V	0.0062	0.0033	0.0152	0.0106	0.0232
Cr	0.0014	0.0017	0.0220	0.0046	0.0227
Mn	0.1619	0.0056	1.1486	0.0120	0.2720
Co	0.0329	0.0422	0.0591	0.0604	0.2087
Fe	5.0565	2.8060	22.6448	6.8116	21.6257
Ni	0.0356	0.0621	0.0511	0.0544	0.0440
Cu	0.0191	0.0412	0.0230	0.0273	0.0270
Zn	0.1342	56.1179	0.1085	1.6770	0.0840
As	0.0059	0.0037	0.0207	0.0050	0.0000
Pb	0.0457	0.0440	0.1137	0.0438	0.0309
W	0.1314	36.2442	0.0993	2.3458	0.0616
Au	0.0000	0.0000	0.0000	0.0000	0.0000
Ag	0.0000	0.0000	0.0000	0.0000	0.0006
Rb	0.0124	0.0000	0.0658	0.0154	0.0659
Nb	0.0002	0.0000	0.0048	0.0056	0.0037
Mo	0.2279	0.0000	0.2346	0.2155	0.2189
Cd	0.0000	0.0012	0.0000	0.0000	0.0000
Sn	0.4545	0.0907	0.5923	0.8107	0.6238
Sb	0.4377	0.0781	0.4964	0.7751	0.5673



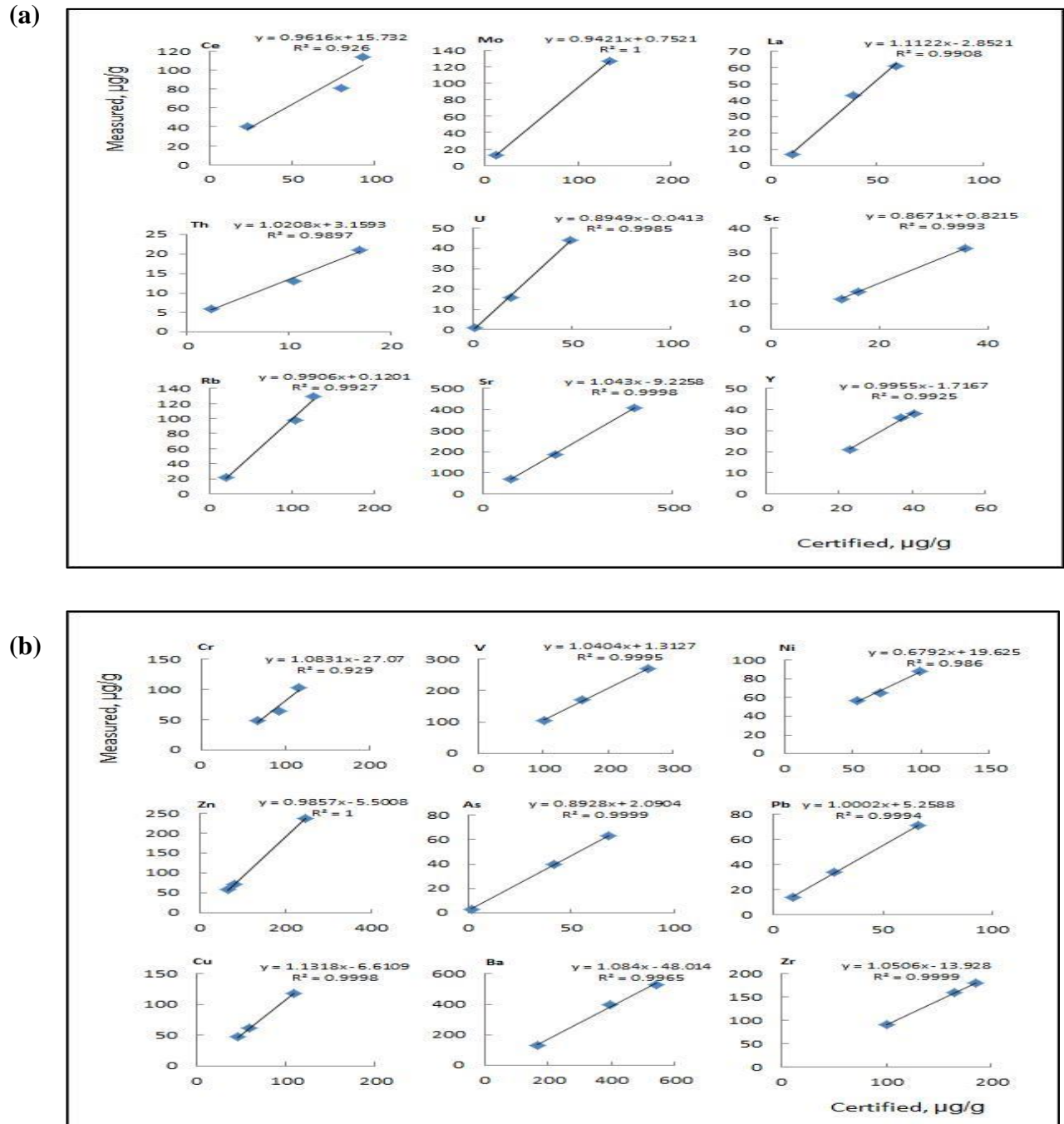


Figure 10: (a & b) Plot of measured versus certified concentrations of trace elements in three certified reference materials: a, SDO-1 (shale, USGS); b, W2a (diabase, USGS); and c, STSD-2 (stream sediment, NRC, Canada). The table of data is presented in Appendix A&B.

The bivariate plots of Figure 10 (a &b) have shown positive and /or strong relationship between the trace elements in the Ameri lodes and their respective certified concentration values which is also The bivariate plots of Figure 10(a &b) have shown positive and /or strong relationship between the trace elements in the Ameri lodes and their respective certified concentration values which is also an indicator that the elements are probably from same hydrothermal source with the Pb-Zn mineralization in the study area.

### Mineralogy, Major Elements Geochemistry

Table 7 present the summary statistics of the concentrations of major and trace elements for the core samples collected from the Ameri lode areas of SE Nigeria. The Table present the results of this work, along with the crustal averages (Andrews *et al.*, 2004; Taylor and McLennan, 1985, 1995; Wedepohl, 1995) and the concentration of the elements in stream sediments from a similar terrane in eastern Nigeria (Lapworth *et al.*, 2012).The data show that for the core samples from Ameri lode area (Table 7, the mean concentrations (wt %) of SiO<sub>2</sub>, TiO<sub>2</sub>, Al<sub>2</sub>O<sub>3</sub> and Fe<sub>2</sub>O<sub>3</sub> are 55.3, 1.1, 8.6 and 4.5 respectively. The results for MgO, CaO, K<sub>2</sub>O and Na<sub>2</sub>O are 0.7, 0.6, 1.8 and 0.3, while MnO and LOI give 0.1 and 4.8 respectively. The results further showed that the mean concentrations of MgO, CaO, K<sub>2</sub>O, Na<sub>2</sub>O, MnO and LOI are like those obtained in AMR 014, AMR 036, and AMR 038 core samples. A major feature of these results is the elevated silica contents and depletion in alumina and the alkalis relative to their published crustal average values (Andrews *et al.*, 2004; Taylor and McLennan, 1985, 1995; Wedepohl, 1995). There is a noticed direct relationship between lead–zinc and sulphur in Ameri lode. Lead combines with sulphur to form most commonly the sulphide and the sulfosalt (Freedman, 1972).

Table 7: Summary of XRF data for major and trace elements in the core samples from Ameri area, SE Nigeria

Elemet	This work			Cont. Crust		
	Min	Max	Mean	A	b*	C
<b>SiO<sub>2</sub></b>	10	59	55.3	65	66	62
<b>TiO<sub>2</sub></b>	0.2	2.9	1.1	0.6	0.5	0.7
<b>Al<sub>2</sub>O<sub>3</sub></b>	3.7	18.1	8.6	15	15	15
<b>MnO</b>	0	0.5	0.1		0.1	0.1
<b>MgO</b>	0.1	6.4	0.5	2.4	2.2	3.7
<b>Fe<sub>2</sub>O<sub>3</sub></b>	1.2	10.5	4.5	4.9	5	6.3

Publication of the European Centre for Research Training and Development -UK

<b>CaO</b>	0.1	5.8	0.7	4.1	4.2	5.5
<b>P<sub>2</sub>O<sub>5</sub></b>	0	1.6	0.24		0.2	0.2
<b>K<sub>2</sub>O</b>	0.4	4.3	1.8	3.1	3.4	2.4
<b>Na<sub>2</sub>O</b>	0	2.4	0.3	3.5	3.9	3.2
<b>LOI</b>	1.6	10.51	4.8			
<b>V</b>	0.0035	0.0195	0.01		60	98
<b>Cr</b>	0	0.0531	0.012		35	126
<b>Ni</b>	0.0273	0.0605	0.044		20	56
<b>Cu</b>	0.0155	0.0412	0.027		25	25
<b>Zn</b>	0.058	58.632 9	14.404		71	65
<b>As</b>	0	2.7717	0.497		1.5	
<b>Rb</b>	0	0.0693	0.017		112	78
<b>Sn</b>	0.1	0.9	0.3		350	333
<b>Sb</b>	0.0336	0.8919	0.262		1.5	
<b>Mo</b>	0	0.2388	0.112		50	84
<b>W</b>	0	37.919 4	9.569		30	30
<b>Au</b>	0	3.0634	0.5659		64	60
<b>Pb</b>	0	66.989 6	11.227		11	8.5

The chemical composition (Table 7) plus the Total Alkalis Vs Silica diagram (Figures 11 and 12) of the samples from the intrusive revealed their basic to ultrabasic nature (Read and Watson, 1977). The phaneritic to micro phaneritic textural properties exhibited by the samples picked from the Ameri environs intrusive as well as the China intrusive suggests their solidification in hyperbyssal

environments. The igneous rocks at the environs are high in alkaline and is suggested to be of common origin, (Figure 12) (Umeji, 1978). The chemistry, texture and colour shows that the underlying igneous rocks of the study area are mainly of basic to ultrabasic clan (gabbro) (Simpson, 1969). This is believed to be a function of fractional crystallization. The ultrabasic parts have very high Total Alkalis Content which is 7.61% and 7.75%.

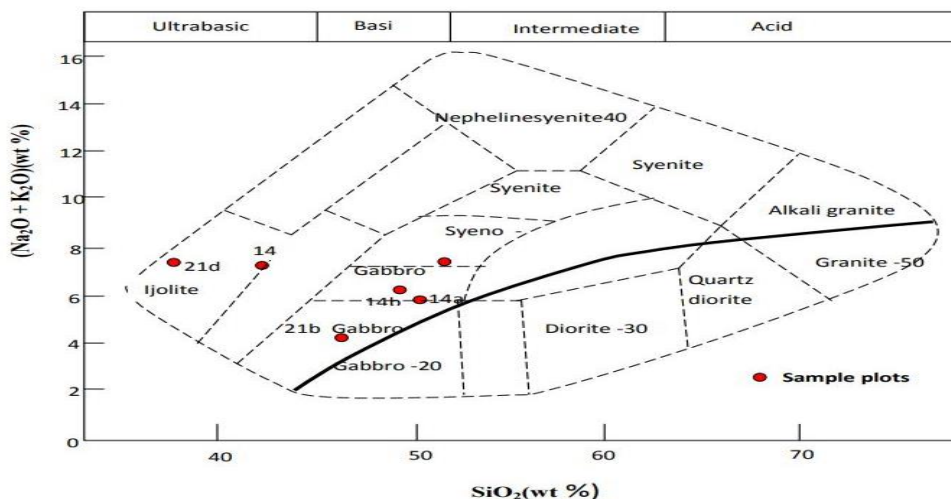


Figure 11: The Chemical Classification of the intrusive rocks using the total alkalis versus silica. (TAS) diagram (Cox et al. 1979). The plot indicates the basic to ultra basic nature of the rocks of the study area.

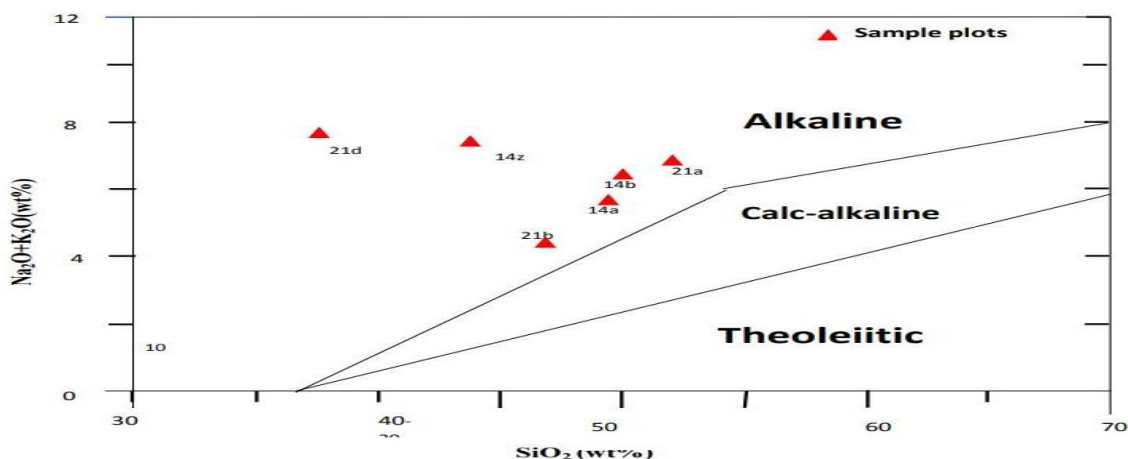
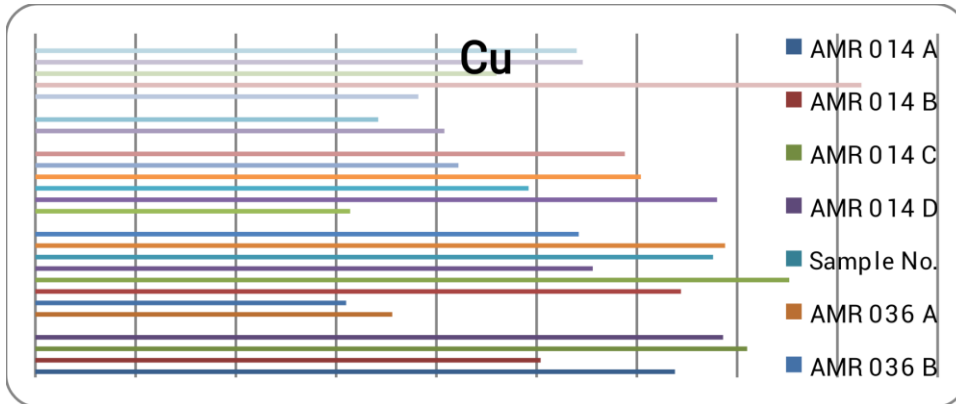


Figure: 12: The total alkalis versus silica (TAS) diagram (After Kuno 1968). The plot indicates that study area is alkaline in nature.



The shear zone contains significant amount of lead, and or zinc. Values of lead within this shear zone ranging from 0.06% - 64.58%, 0.02% - 64.35%, 0.01% - 0.14%, 0.03% - 0.11% for core AMR 036, AMR 038, AMR 048, AMR 049 respectively, while zinc ranges in value from; 0.09% - 53.98%, 0.08% - 1.11%, 0.19% - 58.64%, 0.08% - 56.11%. The value of lead and zinc within the hanging g wall are 0.06% and 0,08%, 0.03% and 0.06%, 0.04% and 0.12%, 0.04% and 0.13% for AMR 036, AMR 038, AMR 048, AMR 049 respectively. Lead and zinc concentrations in the footwall varies from 0.05% - 0.12% and 0.16% - 0.28% in AMR 038 while in AMR 048, the values are 0.14% and 0.05% for lead and zinc respectively. However, AMR 014 which exhibit no shear zone has values ranging from 0.00% - 66.99% and 0.10% - 57.61% for lead and zinc respectively. There is a noticed direct relationship between lead–zinc and sulphur in Ameri lode. Lead combines with sulphur to form most commonly the sulphide and the sulphates (Freedman, 1972). Occasionally, iron is high in some samples with values up to 59.47%.



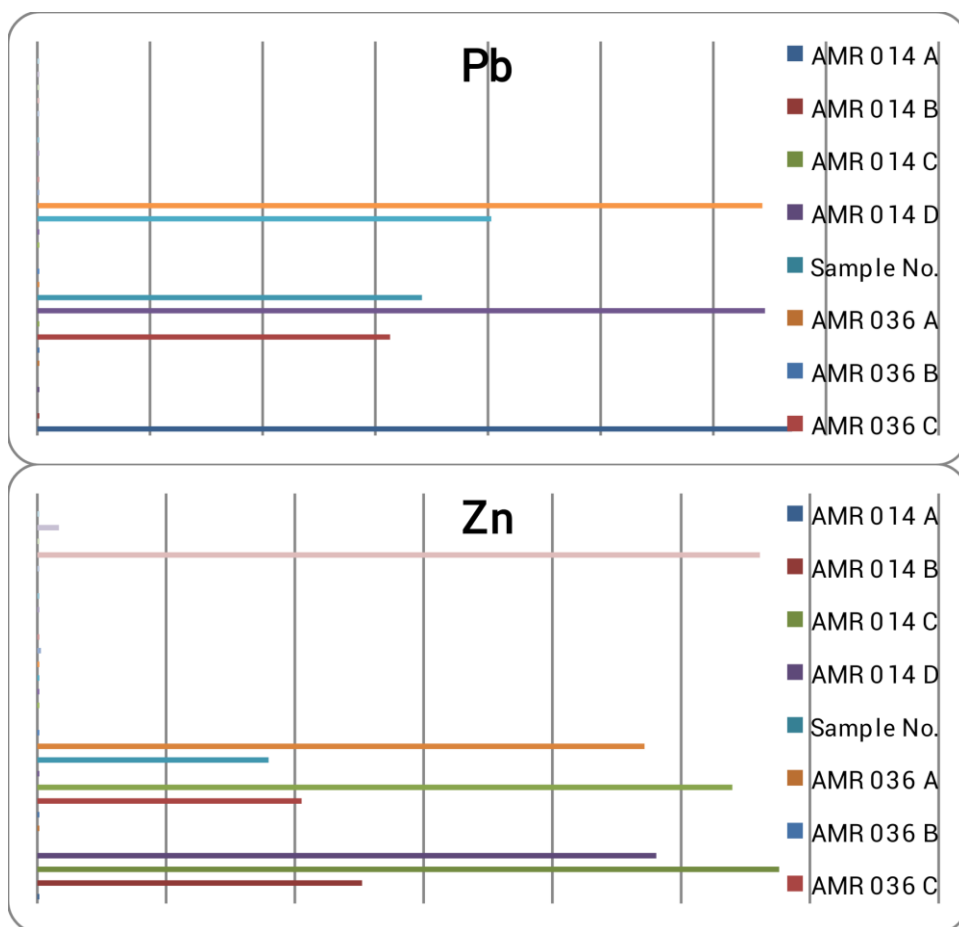


Figure 13: Histograms showing the non-normal nature of the distribution of trace elements data in the samples from the Ameri lode area (AMR 014, 036, 038, 048 & 049)

### Trace Elements Geochemistry

The data shows that the concentration of Pb, Cu, As, Cr and Zn in the Ameri lode samples (Table 2 - 7) ranges from 0 to 66.9896 with a mean of 11.227; 0.0155 to 0.0412 with a mean of 0.027; 0 to 2.7717 with a mean of 0.497; 0 to 0.0531 with a mean of 0.012 and 0.058 to 58.6329 with a mean of 14.404 respectively, while the concentration of Ni ranges from 0.0273 to 0.0605 with a mean of 0.044 %. The concentrations of Pb, Zn and W are very high in the samples AMR 014 (A, B, C & D), 036 (C, D, E & F), 038D compared to those from the AMR 048 and 049 of the study area. Similarly, the mean concentrations of all the above six elements obtained from the Ameri lode samples are far below their crustal concentrations (Taylor and McLennan, 1985, 1995; Wedepohl, 1995), except for Pb which has a mean concentration slightly more than 8.5 (Wedepohl, 1995). In the Ameri lode area, the concentration of S appears to co-vary with those of Zn, and Pb, such that samples with high Zn and Pb levels also have elevated S concentrations (Figure 15). This is perhaps because of associated barite mineralization or the presence of S in carbonate materials.

### Paleo-Redox condition

Hallberg (1976) introduced the use of Cu/Zn and (Cu+Mo)/Zn ratios as redox parameters. He stated that high Cu/Zn ratios indicate reducing depositional conditions, while low Cu/Zn ratios suggest oxidizing conditions in the depositional basins. Low Cu/Zn ratios (0.001-0.324, 0.001 – 0.307, 0.075-0.424, 0.001-0.309 and 0.001-0.321 for AMR 014, AMR 036, AMR 038, AMR 048, AMR 049 respectively) this indicates more oxidizing conditions than reducing. This is also confirmed by the Ni/Co ratio (0.00-58.50, 0.00-43.625, 0.00-35.333, 0.00-1.704, 0.211-1.472 for AMR 014, AMR 036, AMR 038, AMR 048, AMR 049 respectively) mostly below the ratio indicated to be oxic by Dypvik (1984) and Dill (1986) with little anoxic environmental affinity. Ni/Co ratios below 5 indicate oxic environments, whereas ratios above 5 indicate subtoxic and anoxic environments.

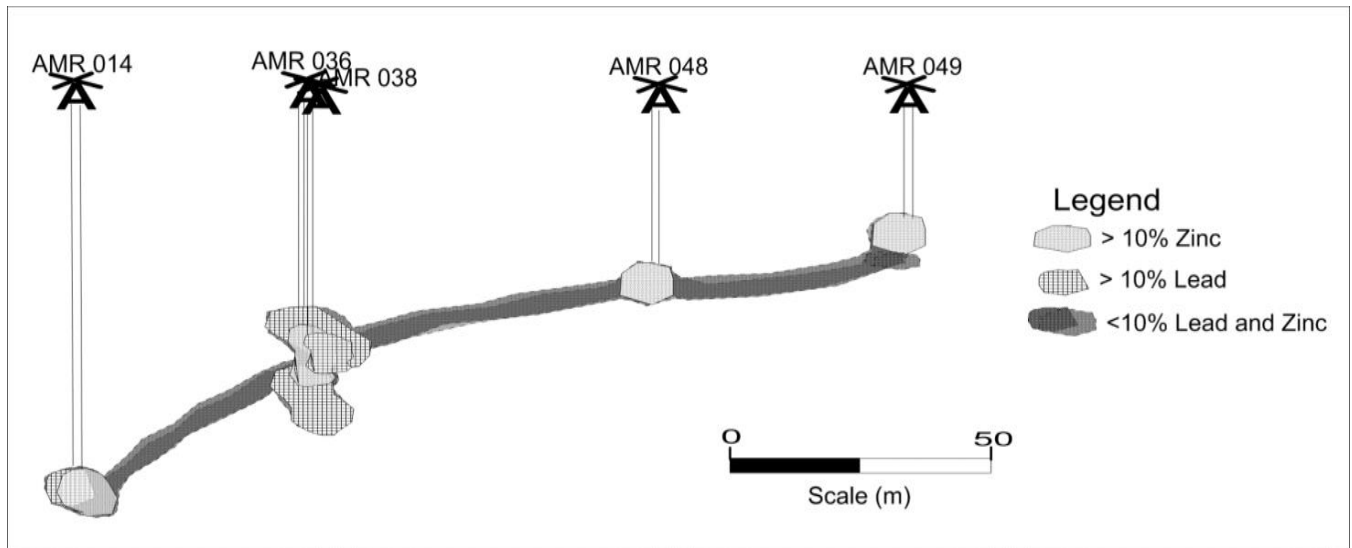


Figure 14: Longitudinal section showing distribution of lead and zinc in Ameri lode, Benue Trough, Nigeria

### CONCLUSION

The geology of the study area is made up of shale intruded by several small to medium sized mesocratic – melanocratic, phaneritic intrusive (basic – ultrabasic igneous rocks) which are alkaline in nature with a slight variation in their mineralogical and textural characteristics. The Lead-Zinc mineralization in the study area is hosted by shales, which are probably parts of the slightly deformed cretaceous sedimentary rocks made up of essentially Albian shales and subordinate siltstones. There is a noticed direct relationship between lead–zinc and Sulphur in Ameri lode. Lead combines with sulphur to form most commonly the sulphide and the sulfosalt (Freedman, 1972). Occasionally, iron is high in some samples with values up to 59.47%. Paleo-redox condition of Low Cu/Zn ratios from the study area indicate more oxidizing conditions than



reducing conditions from the data sets. This is confirmed by the Ni/Co ratio mostly below the ratio indicated to be oxic by Dypvik (1984) and Dill (1986) with little anoxic environmental affinity.

## REFERENCES

1. Akande, S.O and Mucke, A. (1989). Mineralogical, Textural and Paragenetic Studies of the Lead Zinc Copper Mineralization in the Lower Benue Trough (Nigeria) and their Genetic. Impication. *Journal of African Earth Science*. 9 (1) 23-29.
2. Burke, K. C., Dessauvage and Whiteman, A. J. (1970). Geological History of the Benue valley and adjacent areas. In *African Geology Univ. of Ibadan*. Press p. 187-206
3. Cox, K.G., Bell, J.D., & Pankhurst R.J., (1979). *The Interpretation of Igneous Rock*. George Allen & Unwin, London)
4. Dill, H. (1986). Metallogenesis of early Paleozoic graptolite shales from the Graefenthal Horst (Northern Bavaria-Federal Republic of Germany).
5. Dypvik, T., (1986). S, P and Sr Isotope Geochemistry and Genesis of Pb-Zn Mineralization in the Huangshaping Polymetallic Ore Deposit of Solution Hunan Province China.
6. Field, A. (2009). *Discovering statistics using SPSS*, 3rd edition, SAGE London.
7. Freedman, E.E. (1972). Coexisting galena, PbS and sulfosalts: Evidence for multiple episodes of mineralization in the Round Mountain and Manhattan gold district, Nevada. *Canadian Mineralogist* 26, 355-376.
8. Idowu, J.O., Ekweozor, C.M. (1993). Petroleum potential of Cretaceous shales in the Upper Benue Trough, Nigeria. *J Petrol Geol* 21:105–118
9. Kennedy, W.Q. (1965). The influence of basement structure on the evolution of the coastal (Mesozoic and Tertiary) basins. In: *Recent Basins around Africa*. Proceedings of the Institute of Petroleum Geologists Society, London. pp. 35–47
10. King, L.C. (1950). Outline and distribution of Gondwanaland. *Geological Magazine*, 87, 353–359
11. Kogbe, C.A. (1989). *Geology of Nigeria*, 2nd Edition. Rockview Nige Ltd, Jos, 538pp
12. London Taylor, S.R. and McLennan, S.M. (1985). *The Continental Crust: its Composition and Evolution*. Blackwell Scientific Publication, Oxford.
13. Nigeria Geological Survey Agency, (2009): Topographical map of part of Ishiagu SE sheets.
14. Nwachukwu, S.O. (1972). The Tectonic Evolution of the Southern Portion of the Benue Trough, Nigeria. *Geol, Mag.* 109: 411 – 419
15. Nwajide, C. S. (1990). Cretaceous Sedimentation and Paleogeography of the Central Benue Trough, Nigeria. In: Ofoegbu C. O. (Ed.). *The Benue Trough Structure and Evolution*. Friedr Vieweg, and Sohn, Braunschweig, Weisbaden, pp. 19–38
16. Obaje, N. G., Abaa, S. I., Najime, T. and Suh, C. E. (1999). *African Geosciences Review*, 6, pp. 71–82
17. Obaje, N.G., Attah, D.O., Opeloye, S.A. And Moumouni, A. (2006). Geochemical evaluation of the hydrocarbon prospects of sedimentary basins in Northern Nigeria. *Geochemical Journal*, vol. 40, pp. 227 – 243

18. Obaje, N. G. (2009). *Geology and Mineral Resources of Nigeria*. Springer Dordrecht Heidelberg London New York
19. Odebode, M.O. (2010). *Geology of the Benue and Anambra Basins, Nigeria*. Unpublished lectures note, 23p.
20. Offodile, M.E. (1980). A mineral survey of the Cretaceous of the Benue Valley, Nigeria. *Cretaceous Res* 1:101–124 Ofoegbu, C.O. (1985). A review of the geology of the Benue Trough Nigeria. *Journal of African Earth Sciences*, Vol. 3: 283-291
21. Ogunidipe, I.E1. and Obasi, R.A. (2016). *Geology and Mineralization in the Albian Sediments of the Benue Trough, Nigeria*. *British Journal of Earth Sciences Research* Vol.4, No.3, pp.1-15
22. Olade, M. A. (1975). Evolution of Nigerian's Benue Trough (Aulacogen): Tectonic model. *Geological Magazine*, 112, pp. 575 – 583
23. Olade, M.A. (1976). On the genesis of lead-zinc deposit in Nigeria's Benue Rift (Aualcogen): A re-interpretation. *J. Min. Geol.* 13:20-27
24. Orajaka, S., (1965). *The Geology of the Enyigba, Ameri and Ameka, Lead-Zinc Lodes, Abakaliki Division, E. Nigeria, and Geology*.2 (2).65-70.
25. Petters, S. W. (1978). Stratigraphic Evolution of the Benue Trough and Its Implications for the Upper Cretaceous Paleogeography of West Africa, *The Journal of Geology*, 86 (3). 311-322
26. Read H.H., & Watson, J., (1977). *Introduction to Geology* .1. The Macmillan Press Ltd
27. Simpson, B., (1969). *Rocks and Minerals*. Pergamon Press, London. 300
28. Taylor, S.R., McLennan, S.M. (1995). The geochemical evolution of continental crust *Rev Geophysics* 33(2), 241-265.
29. Tijani, M.N., Loehnert, E.P., Uma, K.O. (1997). Origin of saline groundwaters in the Ogoja area, Lower Benue Trough, Nigeria. *J Afr. Earth Sci* 23:237–252
30. Tijani, M.N., Okunlola, O.A., Abimbola, A.F. (2006). Lithogenic concentrations of trace metals in soils and saprolites over crystalline basement rocks: a case study from SW Nigeria. *J. Afr. Earth Sci.* 46, 427-438.
31. Umeji A.C., (1978). *Alkaline Magmatism and Faulting in the Basement Margin of the Benue Trough, Nigeria*. Nigerian Mining and Geoscience Society.
32. Usoro, M. E., Aniefiok E. I., Thomas A. H., Clement E. B. and Edet W. N. (2015). Assessment of Cadmium and Lead Distribution in the Outcrop Rocks of Abakaliki Anticlinorium in the Southern Benue Trough, Nigeria. *Journal of Environment Pollution and Human Health*, Vol. 3, No. 3, 62-69
33. Wedepohl, K.H. (1995). The composition of the continental crust. *Geochim Cosmochim Acta* 59 (7), 1217-1232.
34. World Health Organization (2011). *World report on Disability*. WHO/NMH/VIP/11.01
35. Wright, J.B. (1968). South Atlantic Continental drift and Benue Trough. *Tectonophysics* 6: 301-310
36. Wright, J.B. (1974). High Pressure phases in Nigeria Cenozoic lavas; distribution and setting. *Bull. Volcano.* 34: 833-847

37. Wright, J. B. (1981). Review of the origin and evolution of the Benue Trough in Nigeria. *Earth Evolution Sciences* 2: 98-103